Letter

Two-phonon scattering in nonpolar semiconductors: A first-principles study of warm electron transport in Si

Benjamin Hatanpää, Alexander Y. Choi, Peishi S. Cheng, and Austin J. Minnich*
Division of Engineering and Applied Science, California Institute of Technology, Pasadena, California 91125, USA

(Received 30 August 2022; revised 22 December 2022; accepted 3 January 2023; published 25 January 2023)

The *ab initio* theory of charge transport in semiconductors typically employs the lowest-order perturbation theory in which electrons interact with one phonon (1ph). This theory is accepted to be adequate to explain the low-field mobility of nonpolar semiconductors but has not been tested extensively beyond the low-field regime. Here, we report first-principles calculations of the electric field dependence of the electron mobility of Si as described by the warm electron coefficient β. Although the 1ph theory overestimates the low-field mobility by only around 20%, it overestimates β by over a factor of two over a range of temperatures and crystallographic axes. We show that the discrepancy in β is reconciled by the inclusion of on-shell iterated two-phonon (2ph) scattering processes, indicating that scattering from higher-order electron-phonon interactions is non-negligible even in nonpolar semiconductors. Further, a ∼20% underestimate of the low-field mobility with 2ph scattering suggests that nontrivial cancellations may occur in the perturbative expansion of the electron-phonon interaction.

DOI: 10.1103/PhysRevB.107.L041110

Introduction. Recent advances in the first-principles treatment of charge transport in semiconductors have enabled the calculation of the low-field electrical mobility without any adjustable parameters [1,2]. The method, based on the Wannier interpolation of electron-phonon matrix elements [3,4], allows the Boltzmann equation to be solved on a sufficiently fine grid to ensure converged transport properties. Calculations of low-field mobility have been reported for various semiconductors, including Si [5–7], GaAs [8–10], and others [11–13]. Methodological developments continue to be reported, including an *ab initio* treatment of two-phonon scattering [10] and the quadrupole electron-phonon interaction [14]. A recent work has extended these methods to magnetotransport [15], high-field transport [16], and transport and noise of warm and hot electrons in GaAs [17,18] and holes in Si [19].

The accuracy of first-principles theory has been tested primarily by computing the low-field mobility and comparing to the available experimental data at various temperatures and doping concentrations. The warm electron regime, defined as the regime in which the next-to-leading-order term of the expansion of current density with electric field is non-negligible, is of interest because it contains information on the band-structure anisotropy [20] and energy relaxation [21] not evident in the low-field mobility. The non-Ohmic mobility of Ge and Si beyond the low-field regime was first reported by Shockley [22] and Ryder [23]. Subsequent investigation led to the prediction [24] and experimental observation [25–29] of the anisotropy of the mobility at high electric field in multivalley semiconductors owing to the differential heating of transverse and longitudinal valleys, known as the Sasaki-Shibuya effect. In 1963, Schmidt-Tiedemann reported a theory of the warm electron tensor, showing that in cubic crystals the fourth-rank warm electron tensor can be completely described by two independent components owing to crystal symmetry [20]. The two independent components are denoted β and γ, with β describing the variation of conductivity with electric field and γ the nonparallelism of the current and electric field. Substantial experimental data versus temperature and crystallographic direction are available for both β and γ for electrons in Si [26,27,30–32].

Although scattering by the interaction of an electron with one phonon (1ph) has typically been employed in theoretical and Monte Carlo studies at low field and in the warm electron regime to interpret transport studies, [29,32–35] other experiments suggest a non-negligible role for higher-order processes [36–39]. In Si, two-phonon (2ph) deformation potentials were extracted from second-order Raman spectra [40,41], and calculations of charge transport properties based on these values have indicated that 2ph scattering may make a non-negligible contribution to scattering rates [42–44]. Recent *ab initio* works have reported that two-phonon scattering plays a role in both low-field and high-field transport in the polar semiconductor GaAs [10,18]. Despite these works, the accepted conclusion from *ab initio* studies is that 1ph scattering is sufficient to describe the low-field mobility of nonpolar semiconductors [11]. However, this conclusion has not been extensively tested away from the low-field regime.

Here, we report first-principles calculations of the warm electron tensor in Si. At the 1ph level of theory, both the low-field mobility and β are overestimated, with a marked discrepancy of β at 300 K of over a factor of two. To address this discrepancy, we compute the scattering due to sequential 1ph processes, corresponding to one of the terms at second order in the electron-phonon interaction. The scattering rates are found to be comparable to those of 1ph scattering over a range of energies, and their inclusion eliminates the discrepancy in β. The resulting ∼20% underestimate of mobility suggests that accounting for cancellations of the two second-order terms of

*Corresponding author: aminnich@caltech.edu

the electron-phonon interaction may be necessary to achieve quantitative agreement for both the mobility and β.

Theory and numerical methods. We begin by describing the numerical approach to compute the transport properties of electrons in Si in the warm electron regime. The low-field mobility calculation is now routine and has been extensively described in Refs. [1,2]. In the low-field regime, the carrier temperature equals the lattice temperature and the current density varies linearly with the electric field. The proportionality coefficient is simply σ_0, the linear dc conductivity.

The warm electron regime is defined by electric fields for which the cubic term of the expansion of current density with electric field becomes non-negligible [20]. Mathematically, the current density vector $\mathbf{j}$ in the warm electron regime can be expanded in powers of the electric field of magnitude E as $j_i = E\sigma_0 e_i + E^3\sigma_{iklm}e_k e_l e_m + \cdots$, where e_i are the components of the unit vector in the direction of the electric field along Cartesian axis i and σ_{iklm} is the fourth-rank warm electron conductivity tensor. In cubic crystals, warm electron transport is fully defined by two components of the tensor, β and γ, where $\sigma_{1111} = \sigma_0\beta$ and $\sigma_{1122} = \frac{1}{3}\sigma_0(\beta - \gamma)$. Equivalently, the warm electron tensor can be specified by the values of β along different crystallographic axes.

The warm electron tensor has not been calculated previously by *ab initio* methods. It may be obtained from the first-principles approach described in Sec. II of Ref. [17] to solve the Boltzmann equation in the warm electron regime. Briefly, the Boltzmann equation for a nondegenerate, spatially homogeneous electron gas subject to an applied electric field $\mathcal{E}$ is given by Eq. (2) of Ref. [17]. The electron-phonon scattering matrix is obtained following the standard method involving Wannier interpolation [3] and explicitly constructed into a collision matrix as described in Refs. [17,18]. In the warm electron regime, the reciprocal space derivative of the total distribution function must be computed. The full derivative is evaluated using a finite-difference approximation given in Refs. [3,45]. The Boltzmann equation then becomes a linear system of equations [Eq. (5) in Ref. [17]] that can be solved by numerical linear algebra methods. With the distribution function obtained, the mobility at various electric fields is computed by Brillouin zone integration. Finally, the warm electron coefficient β is obtained by fitting the mobility versus field to a quadratic polynomial as $\mu = \mu_0(1 - \beta E^2)$. We note that β can also be computed via an expansion of the current density in powers of electric field, as shown in the Supplemental Material [46] (see also Ref. [47] therein). We choose the former method for simplicity, although either method is valid. We define the fitting range as that corresponding to a 0.1% increase in electron temperature; the value of β is not sensitive to this choice.

Regarding numerical details, the electronic structure and electron-phonon matrix elements are computed on a coarse $8 \times 8 \times 8$ grid using density-functional theory (DFT) and density-functional perturbation theory (DFPT) with QUANTUM ESPRESSO [48]. We employ a plane-wave cutoff of 40 Ry and a relaxed lattice parameter of 5.431 Å. Once the electronic structure and electron-phonon matrix elements on a coarse grid were computed, they were interpolated on a finer grid of 100^3 using PERTURBO. We set the Fermi level 203 meV below the conduction band minimum (CBM) corresponding to a nondegenerate electron gas of concentration of 10^{16} cm^{-3} at 300 K. The energy window of the Brillouin zone was set to 287 meV above the CBM. Increasing the energy window to 447 meV changed the mobility by 0.1% and β by 0.8%, while increasing the grid density to 140^3 resulted in mobility changes on the order of 1%. The final system of linear equations was solved by a PYTHON implementation of the generalized minimal residual (GMRES) method [49].

As in prior work, spin-orbit coupling is neglected as it has a weak effect on electron transport properties in Si [7,11]. Quadrupole electron-phonon interactions were neglected as they provide only a small correction to the low-field mobility of silicon at room temperature [14].

Mobility and warm electron tensor. Figure 1 shows the computed low-field mobility versus temperature for electrons in Si at the 1ph level of theory. The low-field value at 300 K is 1737 cm^2 V^{-1} s^{-1}, approximately 20% higher than experimental drift mobility values, which range between 1300 and 1450 cm^2 V^{-1} s^{-1} [50–53]. The calculated value at 300 K is generally consistent with prior *ab initio* studies, which report values of 1915 cm^2 V^{-1} s^{-1} [11], 1860 cm^2 V^{-1}s^{-1} [5], and 1750 cm^{2}V^{-1} s^{-1} [6]. The use of the experimental lattice constant and *GW* quasiparticle corrections leads to lower mobility values [7]. The general overestimate of low-field mobility in past *ab initio* studies occurs across a wide range of temperatures, as Refs. [5,11] show an overestimated mobility from 100 to 300 K.

At higher fields, the mobility decreases below the low-field value owing to electron heating as described by β. Because β depends on the direction of the applied field, we denote β without subscripts to indicate the electric field is applied along the [100] crystallographic axis. In Fig. 2(a), we show the mobility versus electric field in the 1ph framework with the electric field applied in the [100] and [111] crystallographic axes along with the quadratic fit. The quadratic fit is observed to agree well with the calculated values. The coefficient of the quadratic fit yields β. The [100] mobility decreases more

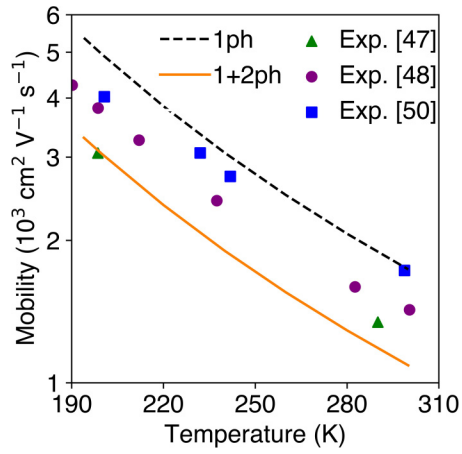

FIG. 1. Low-field mobility vs temperature for the 1ph (dashed black line) and 1+2ph (solid orange line) frameworks. The mobility is overestimated with the 1ph level of theory, but underestimated when including on-shell 2ph scattering. Experimental data: Fig. 11, Ref. [50] (green triangles), Fig. 1, Ref. [54] (purple circles), Fig. 2, Ref. [55] (blue squares).

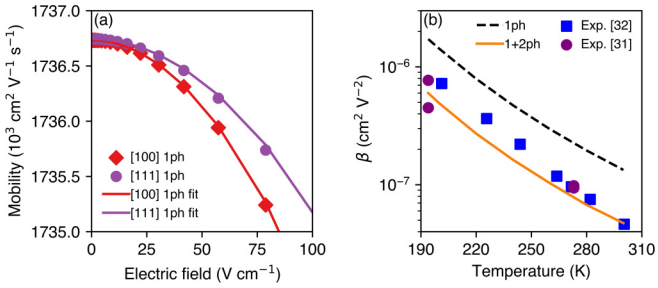

FIG. 2. (a) Mobility vs electric field applied along both the [100] (red diamonds) and [111] (purple circles) crystallographic axes at 300 K using 1ph scattering along with the quadratic fits (solid lines). (b) β vs temperature for the 1ph (dashed black line) and on-shell 2ph (solid orange line) frameworks. β is overestimated by $\gtrsim$100% at the 1ph level of theory across all temperatures. When including on-shell 2ph, the discrepancy is eliminated. Experimental data from Fig. 11, Ref. [32] (blue squares) and Figs. 3 and 4, Ref. [31] (purple circles).

rapidly with field than the [111] case, thus yielding a larger value for β_{100} than β_{111}.

In Fig. 2(b) we compare the computed β versus temperature with experimental data. The prediction from the 1ph level of theory is clearly larger than the experimental values by around 150% across all temperatures. This discrepancy is markedly larger than that of the low-field mobility. Figures 3(a) and 3(b) show β versus angle between current direction and electric field at 300 and 194 K, respectively. Here, the mobility is presented as the field is rotated from the [001] direction (corresponding to 0°) to the [110] direction (corresponding to 90°). While the qualitative trend in β with field orientation seen in experiments is captured by the 1ph theory, the computed results again are greater than experiments by over 100% at both temperatures.

Role of higher-order phonon scattering. Figures 2(b) and 3 indicate that β is markedly overestimated at the 1ph level of theory. The magnitude of discrepancy cannot be easily explained by inaccuracies in band structure, as the discrepancies of the effective mass are ∼7%. Therefore, we

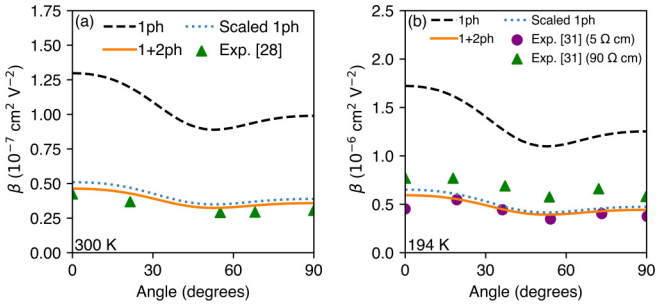

FIG. 3. (a) β vs electric field orientation angle between the [001] and [110] crystallographic axes at 300 K for the 1ph (dashed black line), scaled 1ph (dotted blue line), and 1+2ph (solid orange line) frameworks. The 1ph theory captures the qualitative dependence of β on angle, but the value is overestimated by ∼200%. The discrepancy is reduced to ∼15% with inclusion of on-shell 2ph scattering. Experimental data from Fig. 7, Ref. [28] (upward green triangles). (b) Same as (a) at 194 K. Data from Figs. 3 and 4, Ref. [31] (purple circles and green triangles).

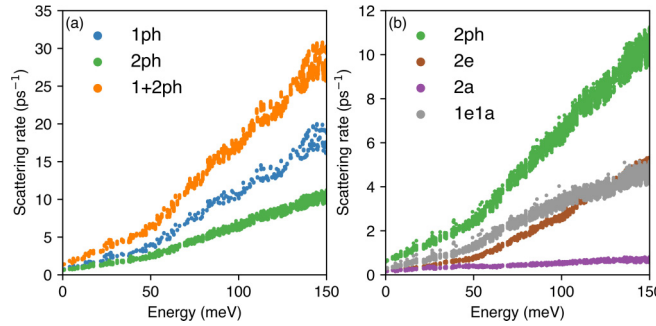

FIG. 4. (a) Computed 1ph (blue), on-shell 2ph (green), and 1+2ph (orange) scattering rates vs energy at 300 K. The on-shell 2ph rates are approximately 50% of the 1ph rates, indicating a non-negligible contribution to transport properties. (b) Computed on-shell 2ph (green), 2e (brown), 2a (purple), and 1e1a (gray) scattering rates vs energy at 300 K. For energies less than 100 meV, the range relevant to transport properties at 300 K, the 1e1a rates are largest and have the dominant effect on transport properties.

considered whether higher-order phonon scattering processes could account for the poor agreement. The 1ph level of theory accounts for the leading-order electron-phonon scattering process for which electrons scatter with one phonon. We implemented a treatment of the next-to-leading-order scattering processes where electrons scatter with two phonons using the *ab initio* approach described in Ref. [10]. As in Ref. [18], beyond the low-field regime the full 2ph calculation is presently computationally intractable, and so we included only on-shell 2ph processes that are within 25 meV of a band energy. Despite the neglect of off-shell processes, Ref. [18] indicates that most of the relevant processes are included with the approximation used here. The 2ph rates were iterated five times.

The computed one- and two-phonon scattering rates are shown in Fig. 4(a). Near the CBM, the 2ph rates are comparable to the 1ph rates. At 100 meV, the maximum energy relevant for transport properties at 300 K, the 2ph rate is approximately 50% of the 1ph rate owing to the weaker energy dependence of 2ph scattering. A disaggregation of the rates into specific emission and absorption processes is shown in Fig. 4(b). For energies less than 100 meV, the 1e1a (one-phonon emission plus one-phonon absorption) rates are the largest and thus have the largest effect on transport properties, while the 2e (two-phonon emission) rates rise once electrons are able to emit two optical phonons. The 2a (two-phonon absorption) rates are relatively negligible at all energies and are only weakly dependent on energy. These characteristics are qualitatively similar to those reported for GaAs in Refs. [10,18].

We now examine the impact of the on-shell 2ph rates on the low-field mobility and β. In Fig. 1, the computed mobility versus temperature including on-shell 2ph scattering is shown. The computed 1+2ph curve underestimates experiment by about 20%. At 300 K, the low-field mobility is 1089 cm^2 V^{-1} s^{-1}. In Fig. 2(b), β including on-shell 2ph scattering versus temperature is shown. With the inclusion of on-shell 2ph scattering, good agreement is observed with two independent experimental reports [29,32]. Similarly, in Fig. 3(a), the agreement with experiment [28] of the

dependence of β on orientation angle at 300 K is greatly improved by including on-shell 2ph. The qualitative trend of a decrease in β from 0° until ∼55° (corresponding to the electric field in the [111] direction), followed by an increase until 90° is unchanged, but it is uniformly decreased in magnitude. The computed β dependence on orientation angle at 194 K shown in Fig. 3(b) lies between two data sets [31] of different resistivities.

We now consider the origin of the improved agreement with β when including on-shell 2ph processes. The first mechanism is the increase in scattering rates, which have a relatively larger effect on β compared to mobility. Specifically, it can be shown that for a uniform scaling of the scattering rates by a factor ϵ, β is scaled by ϵ^{-2} rather than ϵ^{-1} as for the mobility. Therefore, the increased scattering rates contributed by on-shell 2ph processes can account for part of the relatively larger decrease in β. To examine how much of the decrease in β was due to the increased scattering rates, we scaled the 1ph scattering rates by a multiplicative factor so that the resulting low-field mobility was equal to the low-field mobility in the 1+2ph case. The dc mobility versus electric field and β were then calculated. The scaled 1ph results can be seen in Fig. 3. At both 300 and 194 K, the majority (94%) of the decrease in β occurs due to the higher scattering rates. However, the calculated values of β with the actual on-shell 2ph scattering rates are still lower than those predicted from the scaled 1ph rates. This further decrease is due to the larger sensitivity of β to the scattering rate at low energies near the CBM compared to that of the mobility (see Supplemental Material [46]). At these energies, 2ph processes make a relatively larger contribution to the scattering rates than at higher energies, leading to a larger reduction in β than expected based on a uniform increase in scattering rates.

Discussion. We now discuss the finding that multiphonon processes are relevant to transport in nonpolar semiconductors. Previous experiment and modeling works have suggested that 2ph processes could account for deviations in the predicted temperature dependence of the mobility from the 1ph deformation potential theory. In particular, two-phonon deformation potentials were extracted from second-order Raman scattering measurements [40,41], and using these values in transport calculations improved the agreement of both the variation of the low-field mobility and β with temperature [42]. However, these conclusions were subject to uncertainty owing to the semiempirical nature of the scattering rates employed in the modeling. The present work overcomes this limitation using the *ab initio* scattering rates that are free of adjustable parameters, thereby providing firm evidence that multiphonon scattering processes are of importance to low-field and warm electron transport in Si.

We additionally consider the role of other multiphonon processes that have been neglected in the present Letter and their potential impact on the transport properties. First, the addition of the neglected off-shell 2ph processes will further increase the scattering rates and decrease both the mobility and β; however, Fig. 2(a) of Ref. [18] indicates this difference is negligible in GaAs. A more involved complication is the role of the direct 2ph interaction arising from simultaneous interactions with two phonons, in contrast to that arising from two sequential 1ph scattering events considered here. Due to translational invariance, a cancellation occurs for interactions involving long-wavelength acoustic phonons [56], and it has been posited that this cancellation may extend to acoustic phonons beyond this limit [57]. To estimate the magnitude of this cancellation, we removed all two-phonon processes that involve acoustic phonons of energy less than 5 meV and recalculated the low-field mobility. The result is 1261 $\mathrm{cm^2\,V^{-1}\,s^{-1}}$, which is in near-quantitative agreement with experiment. This result indicates that taking into account the cancellation between the two 2ph vertices may be needed for predictive accuracy. Further tests of the role of multiphonon processes may be obtained by calculating the free carrier absorption spectrum using the methods of Ref. [58] and the power spectral density of current fluctuations as in Refs. [17,18].

Summary. We have presented a first-principles calculation of the warm electron transport properties of Si. At the 1ph level of theory that is typically regarded as adequate for nonpolar semiconductors, the low-field mobility is overestimated by around 20% while β is overestimated by over 100% across a wide range of temperatures and crystallographic axes. The discrepancy in β is reconciled by inclusion of 2ph scattering, which is found to exhibit a scattering rate that is comparable to that from 1ph processes. The underestimate of the mobility at this level of theory provides evidence for the occurrence of a nontrivial cancellation of second-order terms in the electron-phonon interaction.

Acknowledgments. B.H. was supported by a NASA Space Technology Graduate Research Opportunity under Grant No. 80NSSC21K1280. A.Y.C., P.S.C., and A.J.M. were supported by AFOSR under Grant No. FA9550-19-1-0321. The authors thank J. Sun, S. Sun, D. Catherall, and T. Esho for helpful discussions.

[1] M. Bernardi, First-principles dynamics of electrons and phonons, Eur. Phys. J. B **89**, 239 (2016).

[2] F. Giustino, Electron-phonon interactions from first principles, Rev. Mod. Phys. **89**, 015003 (2017).

[3] A. A. Mostofi, J. R. Yates, Y.-S. Lee, I. Souza, D. Vanderbilt, and N. Marzari, Wannier90: A tool for obtaining maximally-localised Wannier functions, Comput. Phys. Commun. **178**, 685 (2008).

[4] G. Pizzi, V. Vitale, R. Arita, S. Blügel, F. Freimuth, G. Géranton, M. Gibertini, D. Gresch, C. Johnson, T. Koretsune, J. Ibañez-Azpiroz, H. Lee, J.-M. Lihm, D. Marchand, A. Marrazzo, Y. Mokrousov, J. I. Mustafa, Y. Nohara, Y. Nomura, L. Paulatto *et al.*, Wannier90 as a community code: New features and applications, J. Phys.: Condens. Matter **32**, 165902 (2020).

[5] W. Li, Electrical transport limited by electron-phonon coupling from Boltzmann transport equation: An *ab initio* study of Si, Al, and MoS_2, Phys. Rev. B **92**, 075405 (2015).

[6] M. Fiorentini and N. Bonini, Thermoelectric coefficients of *n*-doped silicon from first principles via the solution of the Boltzmann transport equation, Phys. Rev. B **94**, 085204 (2016).

[7] S. Poncé, E. R. Margine, and F. Giustino, Towards predictive many-body calculations of phonon-limited carrier mobilities in semiconductors, Phys. Rev. B **97**, 121201(R) (2018).

[8] J.-J. Zhou and M. Bernardi, *Ab initio* electron mobility and polar phonon scattering in GaAs, Phys. Rev. B **94**, 201201(R) (2016).

[9] T.-H. Liu, J. Zhou, B. Liao, D. J. Singh, and G. Chen, First-principles mode-by-mode analysis for electron-phonon scattering channels and mean free path spectra in GaAs, Phys. Rev. B **95**, 075206 (2017).

[10] N.-E. Lee, J.-J. Zhou, H.-Y. Chen, and M. Bernardi, Ab initio electron-two-phonon scattering in GaAs from next-to-leading order perturbation theory, Nat. Commun. **11**, 1607 (2020).

[11] J. Ma, A. S. Nissimagoudar, and W. Li, First-principles study of electron and hole mobilities of Si and GaAs, Phys. Rev. B **97**, 045201 (2018).

[12] J. Sun, H. Shi, T. Siegrist, and D. J. Singh, Electronic, transport, and optical properties of bulk and mono-layer $PdSe_2$, Appl. Phys. Lett. **107**, 153902 (2015).

[13] N.-E. Lee, J.-J. Zhou, L. A. Agapito, and M. Bernardi, Charge transport in organic molecular semiconductors from first principles: The bandlike hole mobility in a naphthalene crystal, Phys. Rev. B **97**, 115203 (2018).

[14] J. Park, J.-J. Zhou, V. A. Jhalani, C. E. Dreyer, and M. Bernardi, Long-range quadrupole electron-phonon interaction from first principles, Phys. Rev. B **102**, 125203 (2020).

[15] D. C. Desai, B. Zviazhynski, J.-J. Zhou, and M. Bernardi, Magnetotransport in semiconductors and two-dimensional materials from first principles, Phys. Rev. B **103**, L161103 (2021).

[16] I. Maliyov, J. Park, and M. Bernardi, *Ab initio* electron dynamics in high electric fields: Accurate prediction of velocity-field curves, Phys. Rev. B **104**, L100303 (2021).

[17] A. Y. Choi, P. S. Cheng, B. Hatanpää, and A. J. Minnich, Electronic noise of warm electrons in semiconductors from first principles, Phys. Rev. Mater. **5**, 044603 (2021).

[18] P. S. Cheng, J. Sun, S.-N. Sun, A. Y. Choi, and A. J. Minnich, High-field transport and hot-electron noise in GaAs from first-principles calculations: Role of two-phonon scattering, Phys. Rev. B **106**, 245201 (2022).

[19] D. Catherall and A. Minnich, High-field charge transport and noise in *p*-Si from first principles, Phys. Rev. B **107**, 035201 (2023).

[20] K. J. Schmidt-Tiedemann, Tensor theory of the conductivity of warm electrons in cubic semiconductors, Philips Res. Rep. **18**, 338 (1963).

[21] M. Costato, S. Fontanesi, and L. Reggiani, Electron energy relaxation time in Si and Ge, J. Phys. Chem. Solids **34**, 547 (1973).

[22] E. J. Ryder and W. Shockley, Mobilities of electrons in high electric fields, Phys. Rev. **81**, 139 (1951).

[23] E. J. Ryder, Mobility of holes and electrons in high electric fields, Phys. Rev. **90**, 766 (1953).

[24] M. Shibuya, Hot electron problem in semiconductors with spheroidal energy surfaces, Phys. Rev. **99**, 1189 (1955).

[25] W. Sasaki, M. Shibuya, and K. Mizuguchi, Anisotropy of hot electrons in *n*-type germanium, J. Phys. Soc. Jpn. **13**, 456 (1958).

[26] M. H. Jørgensen, N. I. Meyer, and K. J. Schmidt-Tiedemann, Conductivity anisotropy of warm and hot electrons in silicon and germanium, Solid State Commun. **1**, 226 (1963).

[27] W. E. K. Gibbs, Conductivity anisotropy and hot electron temperature in silicon, J. Phys. Chem. Solids **25**, 247 (1964).

[28] C. Hamaguchi and Y. Inuishi, Conductivity anisotropy of hot electrons in n-type silicon heated by microwave fields, J. Phys. Chem. Solids **27**, 1511 (1966).

[29] M. H. Jørgensen, Warm-electron effects in *n*-type silicon and germanium, Phys. Rev. **156**, 834 (1967).

[30] M. A. C. S. Brown, Deviations from Ohm's law in germanium and silicon, J. Phys. Chem. Solids **19**, 218 (1961).

[31] P. Kästner, E.-P. Röth, and K. Seeger, Conductivity anisotropy of *n*-type silicon in the range of warm and hot carriers, Z. Phys. **187**, 359 (1965).

[32] C. Hamaguchi and Y. Inuishi, Temperature dependence of mobility of warm carriers in germanium and silicon, J. Phys. Soc. Jpn. **18**, 1755 (1963).

[33] E. Conwell, *High Field Transport in Semiconductors* (Academic, New York, 1967).

[34] M. Asche and O. G. Sarbei, Electric conductivity of hot carriers in Si and Ge, Phys. Status Solidi B **33**, 9 (1969).

[35] W. Fawcett, A. D. Boardman, and S. Swain, Monte Carlo determination of electron transport properties in gallium arsenide, J. Phys. Chem. Solids **31**, 1963 (1970).

[36] W. P. Dumke, Two-phonon indirect transitions and lattice scattering in Si, Phys. Rev. **118**, 938 (1960).

[37] P. Thomas and H. J. Queisser, Electron-phonon coupling in the barriers of GaAs schottky diodes, Phys. Rev. **175**, 983 (1968).

[38] R. A. Stradling and R. A. Wood, The magnetophonon effect in III-V semiconducting compounds, J. Phys. C **1**, 1711 (1968).

[39] N. O. Folland, Shapes of two-phonon recombination peaks in silicon, Phys. Rev. B **1**, 1648 (1970).

[40] P. A. Temple and C. E. Hathaway, Multiphonon raman spectrum of silicon, Phys. Rev. B **7**, 3685 (1973).

[41] J. B. Renucci, R. N. Tyte, and M. Cardona, Resonant Raman scattering in silicon, Phys. Rev. B **11**, 3885 (1975).

[42] S. S. Kubakaddi and B. S. Krishnamurthy, The electron-two short-wavelength phonon scattering in non-polar semiconductors, Phys. Status Solidi B **80**, 603 (1977).

[43] K. L. Ngai, Carrier-two phonon interaction in semiconductors, in *Proceedings of the Twelfth International Conference on the Physics of Semiconductors*, edited by M. H. Pilkuhn (Vieweg+Teubner Verlag, Wiesbaden, 1974), pp. 489–498.

[44] G. P. Alldredge and F. J. Blatt, On the role of two-phonon processes in the energy relaxation of a heated-electron distribution, Ann. Phys. **45**, 191 (1967).

[45] N. Marzari, A. A. Mostofi, J. R. Yates, I. Souza, and D. Vanderbilt, Maximally localized Wannier functions: Theory and applications, Rev. Mod. Phys. **84**, 1419 (2012).

[46] See Supplemental Material at http://link.aps.org/supplemental/10.1103/PhysRevB.107.L041110 for a discussion of the energy dependence of mobility and β.

[47] G. Chen, *Nanoscale Energy Transport and Conversion: A Parallel Treatment of Electrons, Molecules, Phonons, and Photons* (Oxford University Press, New York, 2005), pp. 240–260.

[48] P. Giannozzi, S. Baroni, N. Bonini, M. Calandra, R. Car, C. Cavazzoni, D. Ceresoli, G. L. Chiarotti, M. Cococcioni, I. Dabo, A. Dal Corso, S. De Gironcoli, S. Fabris, G. Fratesi, R. Gebauer, U. Gerstmann, C. Gougoussis, A. Kokalj, M. Lazzeri, L. Martin-Samos *et al.*, Quantum Espresso: A modular and open-source software project for quantum simulations of materials, J. Phys.: Condens. Matter **21**, 395502 (2009).

[49] V. Frayssé, L. Giraud, S. Gratton, and J. Langou, Algorithm 842: A set of GMRES routines for real and complex arithmetics on high performance computers, ACM Trans. Math. Softw. **31**, 228 (2005).

[50] C. Canali, C. Jacoboni, G. Ottaviani, and A. Alberigi-Quaranta, High-field diffusion of electrons in silicon, Appl. Phys. Lett. **27**, 278 (1975).

[51] G. W. Ludwig and R. L. Watters, Drift and conductivity mobility in silicon, Phys. Rev. **101**, 1699 (1956).

[52] M. B. Prince, Drift mobilities in semiconductors. II. Silicon, Phys. Rev. **93**, 1204 (1954).

[53] J. Messier and J. M. Flores, Temperature dependence of Hall mobility and μ_H/μ_D for Si, J. Phys. Chem. Solids **24**, 1539 (1963).

[54] P. Norton, T. Braggins, and H. Levinstein, Impurity and lattice scattering parameters as determined from Hall and mobility analysis in *n*-type silicon, Phys. Rev. B **8**, 5632 (1973).

[55] R. A. Logan and A. J. Peters, Impurity effects upon mobility in silicon, J. Appl. Phys. **31**, 122 (1960).

[56] T. Holstein, Theory of ultrasonic absorption in metals: The collision-drag effect, Phys. Rev. **113**, 479 (1959).

[57] P. Kocevar, Multiphonon scattering, in *Physics of Nonlinear Transport in Semiconductors*, edited by D. K. Ferry, J. R. Barker, and C. Jacoboni, NATO Advanced Study Institutes Series Vol. 52 (Springer, Boston, 1980), pp. 167–174.

[58] J. Noffsinger, E. Kioupakis, C. G. Van de Walle, S. G. Louie, and M. L. Cohen, Phonon-Assisted Optical Absorption in Silicon from First Principles, Phys. Rev. Lett. **108**, 167402 (2012).